International Journal for Computational Civil and Structural Engineering, 20(2) 76–87 (2024)

DOI:10.22337/2587-9618-2024-20-2-76-87

NUMERICAL SIMULATION OF THE OPERATION OF ALUMINUM ALLOY JOINTS MADE BY CONTACT CAPACITOR WELDING

Andrey V. Korgin

National Research Moscow State University of Civil Engineering (NRU MGSU), Moscow, RUSSIA

Abstract. Currently, structures made of modern aluminum alloys are increasingly used and widespread in almost all areas of industrial and construction production, which is a consequence of the unique properties of physico-mechanical aluminum alloys, which make it possible to create structures of various purposes that are effective in weight, strength and aesthetic parameters, while having increased corrosion resistance compared to steel structures. However, the manufacture of structures made of aluminum alloys is a more complex technological process due to the need to use special aluminum welding methods compared to traditional methods of welding steel structures. he most common argon arc method and friction welding method with mixing of aluminum alloy structures are more difficult to implement in the field during installation and assembly of structural elements on a construction site, and require qualified personnel. For this reason, it is relevant to use other methods of welding elements of aluminum structures that do not require complex equipment and qualified personnel, similar to classical electric welding of steel structures, compared with the above more complex methods of welding aluminum structures. These technologies include modern methods of laser welding and contact capacitor spot welding, the equipment for which is very compact and mobile and does not require highly qualified personnel as for other aluminum welding technologies. The current regulatory documentation of the Russian Federation on contact capacitor spot welding is descriptive and does not allow reliable design and calculation of the strength of joints of this type, which requires additional experimental and theoretical studies of such joints. Earlier laboratory tests of samples of aluminum alloy compounds by condenser welding showed in some cases a significant difference between experimental data and strength calculations according to the normative methodology of compounds of this type. For this reason, the purpose of this work was to clarify regulatory solutions using numerical FEM modeling of the operation of experimentally tested 18 connections – nodes of the ceiling suspension of aluminum alloy sheets AMG2M to threaded rods made of aluminum alloy AMG3. The obtained data were compared with experimental results and previously performed data of normative calculations.

Keywords: aluminum alloy, spot capacitor welding, tension, shear, stress, strength, fracture, finite element method

ЧИСЛЕННОЕ МОДЕЛИРОВАНИЕ РАБОТЫ СОЕДИНЕНИЙ ИЗ АЛЮМИНИЕВЫХ СПЛАВОВ, ВЫПОЛНЕННЫХ МЕТОДОМ КОНТАКТНОЙ КОНДЕНСАТОРНОЙ СВАРКИ

А.В. Коргин

Национальный исследовательский Московский государственный строительный университет, г. Москва, РОССИЯ

Аннотация. в настоящее время конструкции из современных алюминиевых сплавов находят все большее применение практически во всех сферах промышленного и строительного производства, что является следствием уникальных физико-механических свойств алюминиевых сплавов, позволяющих создавать эффективные по весовым, прочностным и эстетическим параметрам конструкции самого разнообразного назначения, обладающие при этом повышенной коррозионной стойкостью по сравнению со стальными конструкциями. Однако изготовление конструкций из алюминиевых сплавов является более сложным технологическим процессом из-за необходимости применять специальные методы сварки алюминия по сравнению с традиционными методами сварки стальных конструкций. Наиболее распространенные в настоящее время аргонодуговой метод и метод сварки трением с перемешиванием конструкций из алюминиевых сплавов более сложно реализуются в полевых условиях при монтаже и сборке элементов конструкций на строительной площадке, и требуют квалифицированного персонала. По этой причине является актуальным использование иных методов сварки элементов алюминиевых конструкций, не требующих сложного оборудования и квалифицированного персонала аналогично классической электросварке

стальных конструкций, по сравнению с вышеперечисленными более сложными методами сварки алюминиевых конструкций. К данным технологиям следует отнести современные методы лазерной сварки и контактной конденсаторной точечной сварки, оборудование для которой весьма компактно и мобильно и не требует персонала высокой квалификации как для других технологий сварки алюминия. Действующая нормативная документация РФ по контактной конденсаторной точечной сварке носит описательный характер, и не позволяет надежно осуществлять проектирование и расчет прочности соединений данного типа, что требует дополнительных экспериментально-теоретических исследований таких соединений. Проведенные ранее лабораторные испытания образцов соединений алюминиевых сплавов конденсаторной сваркой показали в ряде случаев существенное различие экспериментальных данных с расчетами прочности по нормативной методике соединений данного типа. По этой причине целью настоящей работы явилось уточнение нормативных решений с помощью численного МКЭ моделирования работы экспериментально испытанных 18 соединений – узлов потолочной подвески листов алюминиевого сплава АМГ2М к стержневым резьбовым тягам из алюминиевого сплава АМГ3. Полученные данные сравнивались с экспериментальными результатами и проведенных ранее данными нормативных расчетов.

Ключевые слова: алюминиевый сплав, точечная конденсаторная сварка, растяжение, срез, напряжение, прочность, разрушение, метод конечных элементов

INTRODUCTION

Currently, structures made of modern aluminum alloys are increasingly used and widespread in almost all areas of industrial and construction production. This is a consequence of the unique properties of physical and mechanical aluminum alloys, which allow to create effective in weight, strength and aesthetic parameters of structures for a variety of purposes with increased corrosion resistance compared to steel ones. However, the manufacture of aluminum alloy structures is a more complex technological process due to the need to apply special methods of welding aluminum compared to traditional welding methods of steel structures. The most common at present argon-arc method and friction stir welding methods for aluminum alloy structures are more difficult to implement in the field during installation and assembly of structural elements at the construction site, and require qualified personnel [1,2,3,4,5,6,7,8]. Because of this, it is relevant to use other methods of welding elements of aluminum structures, which do not require complex equipment and qualified personnel similar to the classical electric welding of steel structures, compared to the above mentioned more complex methods of welding aluminum structures. These technologies should include modern methods of laser welding and contact capacitor spot welding, the equipment for which is very compact, mobile and does not require highly qualified personnel [9,10,11,12,13,14].

The current standards of the Russian Federation on contact capacitor spot welding (GOST 15878-79) are descriptive in nature and do not allow reliable design and calculation of the strength of this type of joints, which requires additional experimental and theoretical studies of such joints.

Previous laboratory tests of samples of aluminum alloy joints performed using condenser welding have shown in a number of cases a significant difference between experimental data and strength calculations according to the normative methodology for joints of this type. For this reason, the purpose of this study was to clarify the normative solutions by means of numerical FEM simulation of the experimentally tested 18 assemblies which are the joints of ceiling suspension of aluminum alloy sheets AMG2M to threaded tie rods made of aluminum alloy AMG3. The obtained data were compared with experimental results and earlier data of computations. Examples of similar studies in Russia and abroad are also given in [15,16,22,23].

The main stages of the study are as follows:

- development of FEM-models of the tested assemblies based on the data of experimental studies conducted earlier;

- numerical modeling of stress-strain state changes during tensile and shear tests of two types of assembly specimens;
- comparing the results of numerical modeling with experimental data and results of verification calculations performed by normative methods in order to be able to correct normative calculation methods for the design of similar assemblies and for the determination of the values of fracture loads;
- drawing conclusions and recommendations on the general calculation of assemblies of this type.

RESEARCH METHODS

Laboratory testing of joints

Previously, there were tested two types of specimens in NIU MGSU which involves joints of plates with dimensions 100×100 mm made of 3 mm thick sheet metal and parts of rolled Taurus with dimensions 100×70×70 mm made of aluminum alloy AMG2M. Studs with internal thread M4 made of aluminum alloy AMG3 were welded to these joints by the method of spot condenser welding [17].

The number of specimens of each type is 9 pieces, total 18 pieces (Fig. 1).

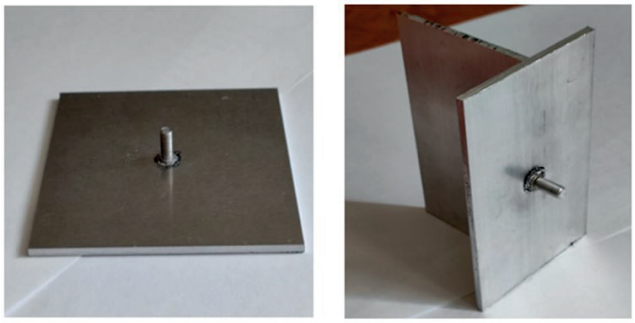


Figure 1. General view of tensile and shear test samples

The joints were subjected to tensile tests with a concentrated force perpendicular to the plane of the plates (type 1), and shear tests by concentrated force parallel to the plane of the plate flange (type 2). The tests were carried out in a universal testing machine Instron 3382 under static loading (Fig. 2) [18].

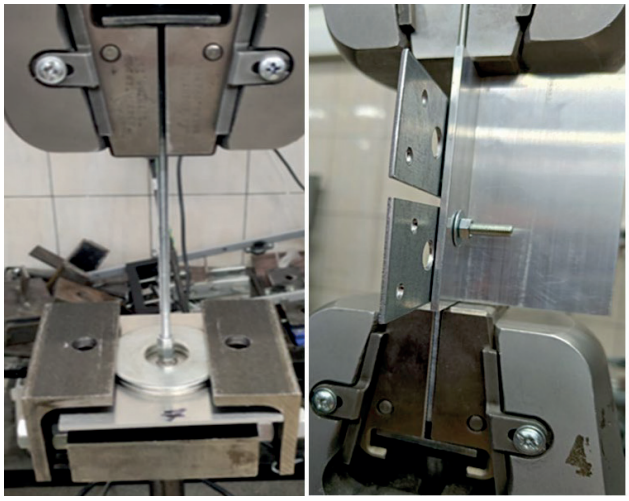


Figure 2. General view of the tensile and shear test samples in the testing machine

Joint strength calculations

In the course of earlier studies, the tested assemblies were subjected to verification calculations according to the standard methodology [17].

Within the framework of the present study, numerical FEM modeling of the tested joints was performed to improve the accuracy of calculations in comparison with the standard methodology and to compare the results of numerical analysis with the results of previously conducted laboratory tests.

RESULTS AND DISCUSSION

Tensile tests

The tensile tests with concentrated tensile force result in failure of the specimens solely by welding (Fig.3).

t



Figure 3. Type of destruction in the welded zone during tensile tests

The results of tensile tests are presented in Table 1. Evaluation of the mean values of failure load obtained was made both without rejection and with rejection of the value for specimen No. 9 due to the deviation from the mean value by more than 50%.

Table 1. Destructive forces during tensile tests.

Sample№	Maximal force, kN	Deviation from average value %	
		Before rejection	After rejection
1	1.68	-19	-17
2	2.32	13	14
3	1.75	-15	-14
4	1.63	-21	-20
*5	2.90	41	42
6	2.41	17	18
7	1.74	-16	-15
8	1.86	-10	-9
***9**	**0.74**	**-64**	**-**
Average value before rejection			**2.06**
Standard deviation			0.608
Coefficient of variation			32%
Average value after rejection			**2.04**
Standard deviation			0.457
Coefficient of variation			22%

* – samples subjected to rejection.

Shear tests

Similarly, shear tests of specimens show that the failure of this type of joints also occurred only by welding (Fig.4).



Figure 4. View of Type 2 samples after the shear tests

The results of the shear tests of the specimens are presented in Table 2.

Table 2. Destructive forces during shear tests.

Sample №	Maximal force, kN	Deviation from average value %	
		Before rejection	After rejection
1	14	26	14
2	-6	4	-6
3	-21	-12	-21
4	0.5	11	0.5
*5	5	15	5
6	-	-72	-
7	0.9	18	0.9
***8**	-	-	-
9	7	18	7
Average value before rejection			**2.08**
Standard deviation			0,608
Coefficient of variation			32%
Average value after rejection			**2.29**
Standard deviation			0.25
Coefficient of variation			11%

* – samples subjected to rejection.

Verification calculations

Tensile and shear test calculations of the two types of joints were performed based on the provisions of SP 128.13330.2016 “Aluminum structures”.

Dimensions of threaded rod M4 PT according to DIN EN ISO 13918 (Fig.5) are as follows:

Diameter of the welding zone (D1+0.5 mm) D_{sv}=6 mm.

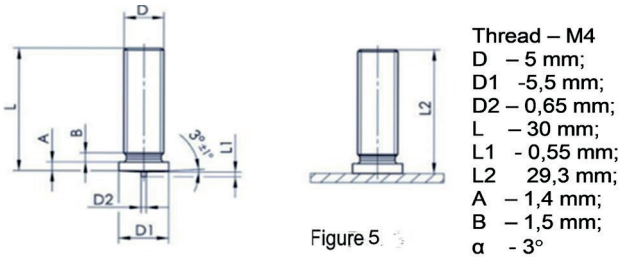


Figure 5. Geometric dimensions of the welded studs. Diameter of welding zone (D_1+0,5 mm) D_w=6 mm. The area of the welding zone A=28.3 mm^2.

Strength properties of the aluminum alloys used in the tested assemblies are given in accordance with the current standards (GOST 21631-2019 “Sheets of aluminum and aluminum alloys”, SP

128 and materials [19] with rounding to 5 MPa (Table 3)).

Table 3. Strength parameters of aluminum alloys

Node element	Tension[MPa]		Shear (срез) [MPa]	
	Yield strength $\sigma_{0,2}$	Maximum resistance $\sigma_в$	Yield strength $\tau_{0,2}$	Maximum resistance $\tau_в$
Plate АМГ2М	70	125	55	90
Threaded stud АМГ3	100	165	70	115

CALCULATION OF TENSILE STRENGTH

Experimental values of normal tensile stresses are presented in Table 4.

Table 4. Normal tensile stresses during tension

Sample №	P (kN)	δP (%)	σ (Pa)	δσ (%)	$\delta\sigma_B$ (%)
1	1,68	-17	5,94E+07	-17	-26
2	2,32	14	8,20E+07	14	2
3	1,75	-14	6,18E+07	-14	-23
4	1,63	-20	5,76E+07	-20	-28
5	2,90	42	1,02E+08	42	28
6	2,41	18	8,52E+07	18	6
7	1,74	-15	6,15E+07	-15	-23
8	1,86	-9	6,57E+07	-9	-18
Average	**2,04**	**0**	**7,20E+07**	**0**	**-10**

Stress in the weld zone for the mean value of fracture force P=2.04 kN:

$$\sigma = \frac{P}{A} = \frac{2{,}04 \cdot 10^3}{28{,}3 \cdot 10^{-6}} = 72 \cdot 10^6 = 72\ MPa < \sigma_B = 80\ MPa\ (\delta = -10\%)$$

Fracture stress range.
σ=68,5÷122 MPa (deviation from σ_B -±28%)

CALCULATION FOR SHEAR

Experimental values of shear tangent stresses are given in Table 5.

Table 5. Shear stresses during cutting

Sample №	P (kN)	δP (%)	τ (Pa)	δτ (%)	$\delta\tau_B$ (%)
1	2,61	14	9,22E+07	28	54
2	2,16	-6	7,63E+07	6	27
3	1,82	-21	6,43E+07	-11	7
4	2,3	0	8,13E+07	13	35
5	2,39	4	8,45E+07	17	41
6	2,31	1	8,16E+07	13	36
7	2,44	7	8,62E+07	20	44
Average	**2,29**	**0**	**8,09E+07**	**12**	**35**

Tangential stress in the weld zone for the mean value of fracture force P=2.29 kN:

$$\sigma = \frac{P}{A} = \frac{2{,}29 \cdot 10^3}{28{,}3 \cdot 10^{-6}} = 80{,}9 \cdot 10^6 = 80{,}9\ MPa > \sigma_B = 55\ MPa\ (\delta = 35\%)$$

Fracture stress range:.
τ=64,3÷92,2 MPa (deviation from τ_B 7÷54%)/

COMPUTER SIMULATION

Strength and deformation properties accepted in the modeling

Strength properties of aluminum alloys are presented in Table 3.
Deformation properties of materials are given in accordance with SP 128 and SP 16.13330.2020 “Steel structures”:
for aluminum alloys:
modulus of elasticity – E=0,7·10^6 MPa;
Poisson's ratio – γ=0,3;
for steel:
modulus of elasticity – E=2,1·10^6 MPa;
Poisson's ratio – γ=0,27.
FEM modeling was conducted in the ANSYS software [20] within the nonlinear elastic-plastic formulation using conventional bilinear elastic-plastic deformation diagrams of the aluminum alloys with regard to [21] (Fig. 6).

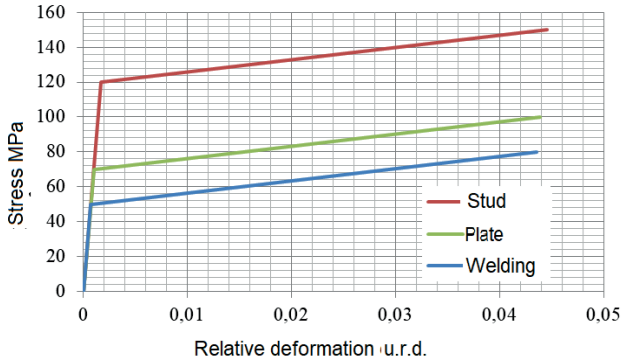


Figure 6. Conditional bilinear diagrams deformations

During modeling, the loading was carried out in stages up to the maximum value of the loading force of 3000 N, which exceeds the values of the failure force achieved during the experiment with a reserve.

Finite elements used

During modeling the SOLID 185 finite elements were used, which represents a three-dimensional three-dimensional cone element with 8 nodes, three degrees of freedom in each (Fig.7).

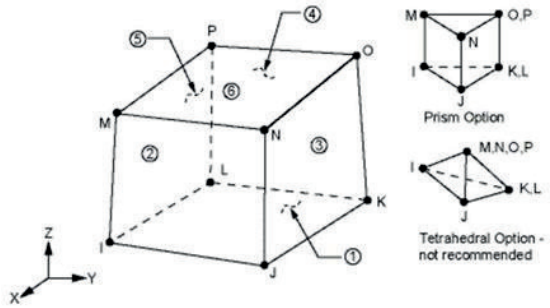


Figure 7. Solid 185 element

The numerical model of the tensile specimen is presented in Fig. 8.

The numerical model of the specimen tested in tension is a spatial model consisting of 4 zones: a stud, a plate, a welded zone made of the aluminum alloys used, and a steel base plate with a circular outline. In accordance with the test design, support was applied along the inner contour of the steel backing plate. The load was applied at the level of the top section of the stud.

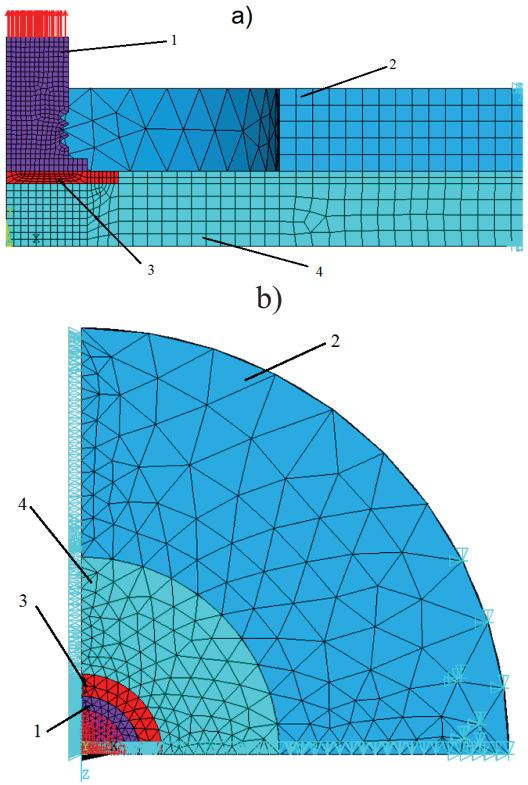


Figure 8. Numerical model of the sample a) front view; b) top view

Based on the symmetry of the model geometry and the applied load, the calculation was performed for ¼ of the model with the corresponding conditions of fixation of the sides of ¼ of the model along the symmetry axes (Fig. 8).

Results of tensile modeling of type 1 specimen.

Isopoles of vertical displacements [mm] are presented in Fig. 9.

The graph of displacements of the center point of the stud surface is shown in Fig.10.

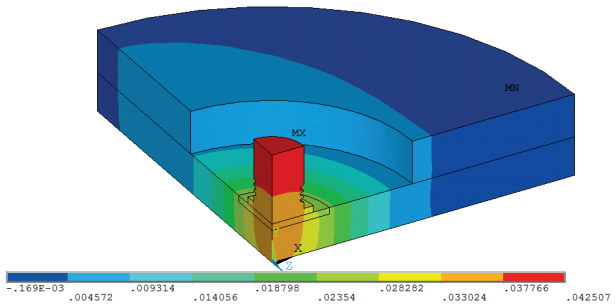


Figure 9. Isofields of vertical movements of the model at a load of 1800 N

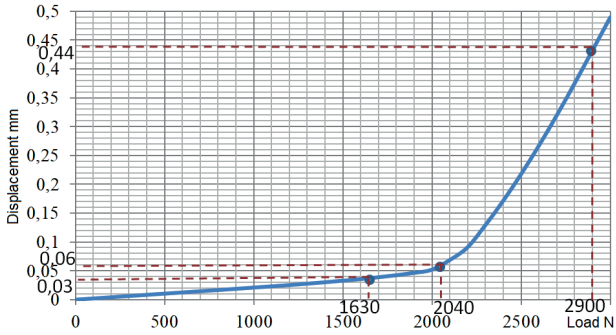


Figure 10. Movements of the upper point of the stud at minimum (1630 N), average (2040 N), and maximum (2900 N) load [mm]

Strains [u.r.d.] and normal stresses [MPa]

The isopoles of strain [u.r.d.] and normal stress[MPa] are shown in Fig. 11:

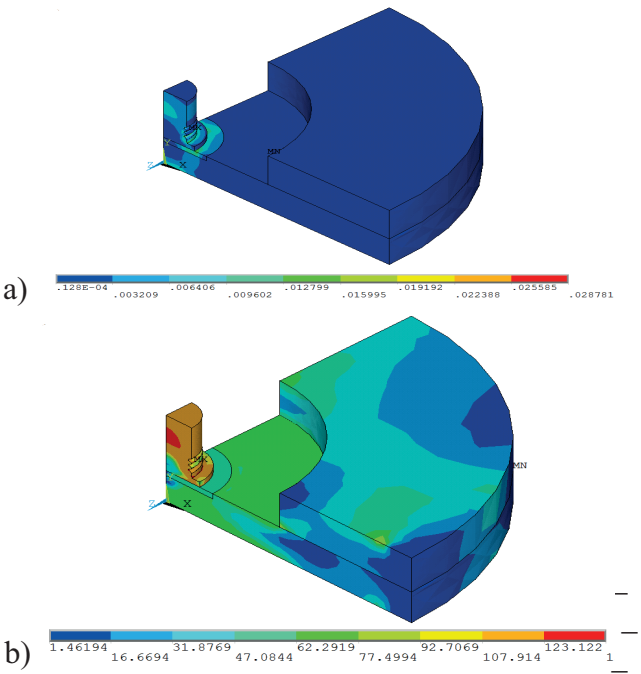


Figure 11. Isofields of a) – deformations, b) – stresses at a load of 1800 N

Fig. 12 shows the graphs of strain in the joint elements and their maximum values at characteristic levels of axial load.

Strain levels in joint elements at recorded values of failure load:

– 0.005 – at minimum load value – 1.63 kN,
– 0.01 – at an average load – 2.04 kN,
– 0.042 – at maximum load value – 2.9 kN.

Relation of maximum values of normal stresses σ in the elements of the node of type 1 to the load is presented in Fig. 13.

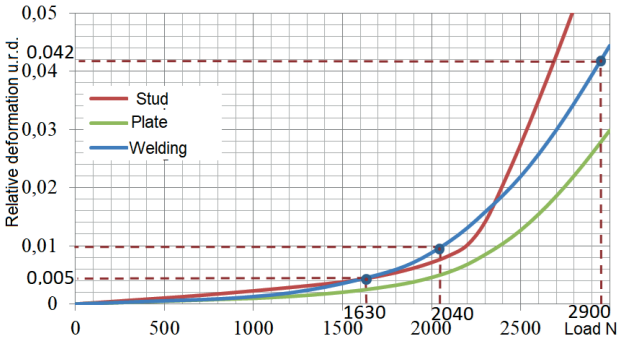


Figure 12. Dependence of the maximum values of relative deformation in the elements of the type 1 node on the load

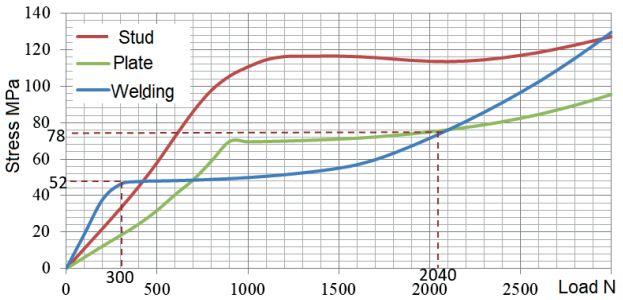


Figure 13. Dependence of the maximum values of normal stresses in the elements of the type 1 node on the load

There is a good correlation between the calculated values of normal stresses in the welding zone and the strength parameters of this zone:

– at the reaching of the yielding point σ=52 MPa ($\sigma_{0.2}$=55 MPa);
– at the value of failure load 2.04 kN – σ=78 MPa (σ_B=80 MPa).

Numerical model of type 2 shear specimen (Fig. 14)

The numerical model of the specimen being tested for shear is a spatial model fixed along the contour and loaded with a concentrated load at a node on the side surface of the stud by means of rigid inserts (MPC).

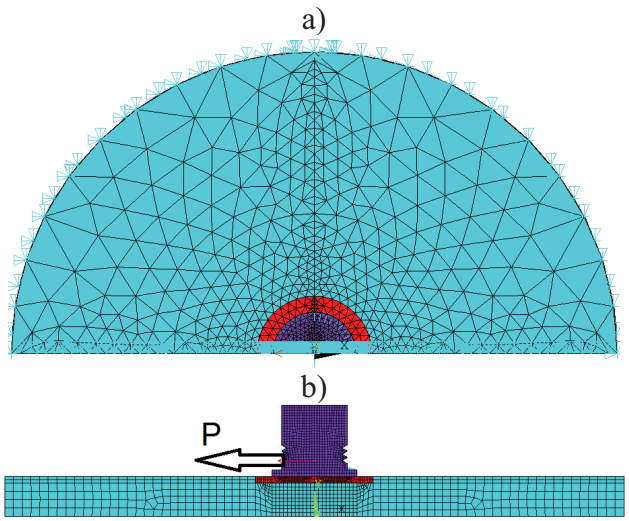


Figure 14. Numerical model of the type 2 sample on a slice: a) top view; b) side view

Based on the symmetry of the specimen geometry and the applied load in one plane, the calculation was performed for ½ of the model with symmetrical fixation along the symmetry axis. The force is applied in the horizontal direction along the symmetry axis.

Results of shear modeling of type 2 specimen

Horizontal displacements [mm] are shown in Fig. 15:

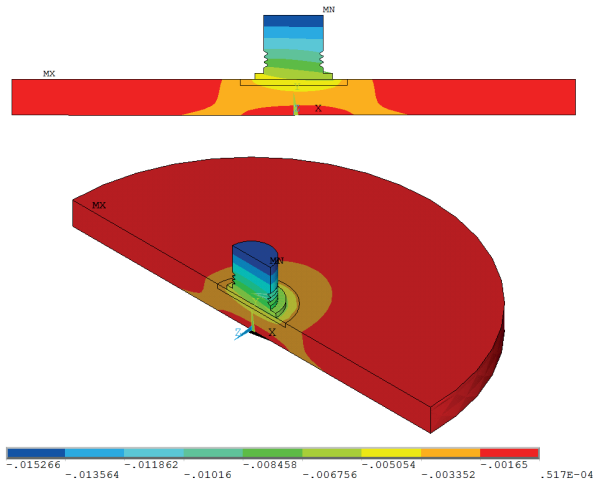


Figure 15. Isofields of horizontal model displacements at a load of 1000 N

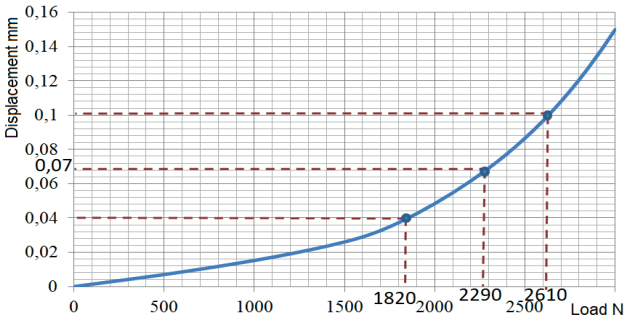


Figure 16. Horizontal movement of the upper point of the stud from the load

Strains γ [u.r.d] and tangential stresses τ [MPa]

The distribution of shear strains and stresses is shown in Figure 17.

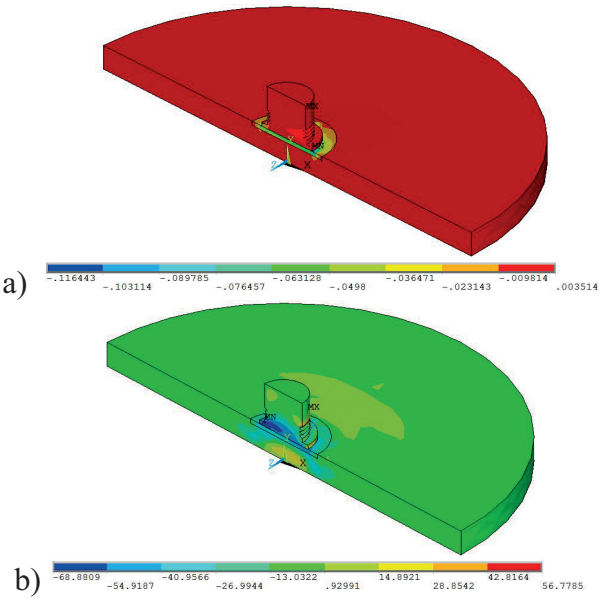


Figure 17. Isofields of a) deformations and b) stresses at a load of 2000 N

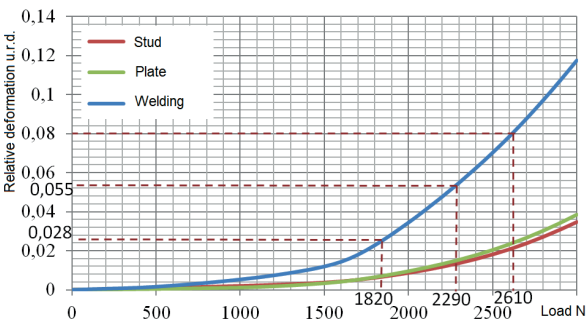


Figure 18. The dependence of the relative deformation in the elements of the type 2 node on the load

The relationship between the maximum values of tangential stresses τ in the elements of the node of type 2 and the load is shown in Fig. 19.

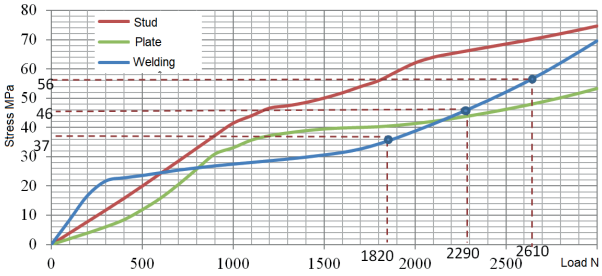


Figure 19. Dependence of the maximum tangential stresses in the elements of the type 2 node on the load

There is a satisfactory correlation of calculated values of tangential stresses τ in the welding zone with strength parameters of this zone in the range of experimental failure loads:
τ=37 MPa for P_{min}=1,82 kN;
τ=46 MPa for P_{cp} =2,29 kN; (δ=16%);
τ=56 MPa for P_{max}=2,61 kN; (τ_B=55 MPa),

CONCLUSIONS AND RECOMMENDATIONS BASED ON COMPARISON OF EXPERIMENTAL RESULTS, VERIFICATION CALCULATIONS AND FEM MODELING

1. Test results

1.1. According to the test results, all specimens of types 1 and 2 were failed along the welded zone.
1.2. The tensile failure force of the joint of type 1 lies within the range of 1.68÷2.9 kN, the mean value is 2.04 kN, the deviation from the mean value is within the range of -20÷+42%.
1.3. The failure force of the joint of type 2 at shear lies within the limits of 1.68÷2.9 kN, the mean value is 2.29 kN, the deviation from the mean value is within the limits of -11÷+20%.

2. Results of verification calculations

2.1. The discrepancy between the results of the calculation of tensile strength and the experiment is satisfactory. It lies within ±28%, from 59.4 MPa to 102 MPa, the mean value is 72 MPa. The average deviation from the tensile strength value of 80 MPa is δ = -10%.
2.2. The discrepancy between the results of the calculation for shear and the experiment is more significant than for tensile. It lies within the range of 7÷54%, from 64.3 MPa to 92.2 MPa. The mean value is 80.9 MPa. The average deviation from the value of shear time resistance 55 MPa is δ=35%.
2.3. The significantly greater difference between the results of calculations for shear and experiment than for tension is a consequence of the more complex actual stress state when the joint is loaded by the shear force caused by the design of the joint than for pure shear. For this reason, the shear performance of the type 2 joint, as well as the tensile performance of the type 1 joint, was analyzed using FEM modeling.

3. Results of FEM modeling

3.1. In tensile testing of type 1 assemblies, there is a good correlation between the calculated values of normal stresses in the weld zone at fracture and the strength parameters of the zone, with the mean value of the failure load kN - σ=78 MPa at σ_B =80 MPa, δ=4%, (with manual calculation δ=10%).
3.2. In shear tests of type 2 assemblies, there is a satisfactory correlation between the calculated values of tangential stresses in the weld zone at fracture and the strength parameters of the zone at an mean value of the failure load of 2.29 kN - τ=46 MPa at τ_B =55 MPa, δ=16% (with manual calculation δ=35%).
3.3. FEM-modeling provides a significantly better match between the results of calculations and experimental results than manual calculations due to more efficient analysis of the actual stress-strain state of the assemblies.
3.4. The design of such nodal joints of aluminum alloys, planned to be performed by means of contact welding, should be carried out on the basis of the results of computer simulation of the joint performance of the constituent elements of the joints under the action of load.

REFERENCES

1. **Shavnev A.A., Kurbatkina E.I., Kosolapov D.V.** Methods of joining aluminum composite materials (review) // Materials and technologies, 2017, No. 3 (48), pp. 35-42.
2. **Krylov D.S., Nazarov S.V.** Some features of argon arc welding of aluminum-magnesium alloys // In the collection: Actual problems of aviation and cosmonautics, Collection of materials of the VI International Scientific and Practical Conference dedicated to the Day of Cosmonautics, in 3 volumes under the general editorship of Yu.Yu. Loginov, 2020, pp. 466-467.
3. **Drits A.M., Ovchinnikov V.V.** Weldability and properties of welds of high-strength aluminum alloys of the Al - Cu - Li system // Metal Science and Heat Treatment, 2012, V. 53, No. 9-10, p.p. 445-449.
4. **Ovchinnikov V.V., Drits A.M.** Welding friction with mixing of aluminum alloys with additional cooling of the joint // Electrometallurgy, 2021. No. 10, pp. 2-14.
5. **Ovchinnikov V.V., Berezina V.A., Skakova T.Y.** Mechanical properties of aluminum alloy joints made by friction welding with static and dynamic loading // High-tech technologies in mechanical engineering, 2021, No. 11 (125), pp. 20-29.
6. **Laptev E.A., Mikhailitsyn S.V., Belyaev A.I.** Friction welding with mixing of aluminum alloys // Actual problems of modern science, technology and education, 2013, Vol. 1, No. 71. pp. 377-379.
7. **Drits A.M., Ovchinnikov V.V.** Properties of the joints of sheets of 1565ch alloy in combination with other aluminum alloys that were performed by friction welding with mixing // Russian Metallurgy (Metally), 2016, V. 2016, № 6, p.p. 537-546.
8. **Amirov A.I., Beloborodov V.A., Ivanov A.N., Zhukov L.L.** Lap welded joint of aluminum and titanium alloy by friction stir welding // Collection of AIP Conference Proceedings, Proceedings of the Advanced Materials with Hierarchical Structure for New Technologies and Reliable Structures, 2018, 020013.
9. **Milyutin V.S., Bliznik M.G. Kataev R.F.** Theory and technology of contact welding // Yekaterinburg, Ural University Publishing House, 2015, 255 p.
10. **Malikov A.G., Orishich A.M., Vitoshkin I.E., Karpov E.V., Ancharov A.I.** Laser welding of heterogeneous materials based on thermally hardened aluminum alloys // Applied Mechanics and Technical Physics, 2021, Vol. 62, No. 5 (369), pp. 161-171.
11. **Wang Z., Shao X., Bu X., Oliveira J.P., Zeng Z., Peng B.** Laser beam oscillating welding of 5a06 aluminum alloys: microstructure, porosity and mechanical properties // Optics & Laser Technology, 2019, V. 11, p.p. 58-65.
12. **Kuchuk A.V.,-Yatsenko S.I., Chvertko P.N., Semenov L.A., Gushchin K.V., Sabotryasov S.M.** Contact butt welding of products made of high-strength alloys based on aluminum // Automatic welding, 2013, No. 7 (723), pp. 3-7.
13. **Chvertko P.N., Semenov L.A., Gushchin K.V.** Contact butt welding by melting thin-walled profiles from thermally hardened aluminum alloys // Automatic welding, 2014, No. 12 (738), pp. 37-40.
14. **Dimitrescu A., Alecusan A.M., Babiş C., Chivu O., Ungureanu L.** Alternative non-demountable assembly technologies for aluminum alloy // In collection of 18th International Multidisciplinary Scientific GeoConference SGEM 2018., Conference proceedings, 2018, pp. 17-24.
15. **Gureeva M.A., Grushko O.E., Klochkov G.G.** Investigation of the properties of welded joints of aluminum alloy B1341 made by contact spot welding // Procurement production in mechanical engineering. 2016, No. 7, pp. 8-12.
16. **Hasan I.Kh ., Pan'kin N.A., Kyashkin V.M.** Xrd study of the surface of aluminum alloy AK5M7 after electric-spark alloying //

Letters about materials, 2021, V. 11. No. 1 (41), pp. 84-89.
17. **Korgin A.V.** Strength of aluminum alloy joints made by contact capacitor welding Vol. 19 No. 2 (2023): International Journal for Computational Civil and Structural Engineering, pp. 42-50.
18. Universal electromechanical machine Instron 3382, User Manual, Instron, USA, 2015, 235 p.
19. **NIL IIMSK NIU MGSU** Technical report for JSC Rusal TD "Development of a set of rules "Bridges with structures made of aluminum alloys. Design rules // NRU MGSU, Moscow, 2020, 230 p.
20. **WWW.Ans.Com.ru** Руководство по основным методам проведения анализа в программе ANSYS, https://vestnik.bsau.ru/netcat_files/File/CIT/manuals/ANSYS.pd, pp. 15-111.
21. **Anisimov A.G., Ahmed S.M.** Experimental investigation and numerical modeling of aluminum sample throwing for magnetic pulse welding // Nauka i innovatsii, 2022, No. 3 (123), pp. 58-62.
22. **Maksimov N.N., Sergeev V.Y**. Improving the technological process of contact welding of aluminum alloy parts // Alley of Science, 2017, Vol. 4, No. 10, pp. 150-157.
23. **Andreeva L.P., Ovchinnikov V.V., Sidorov A.A.** Optimization of point joint sizes during electric contact welding of aluminum alloys // Modern Materials, Technique and Technology, 2015, No. 3 (3), pp. 23-32.

СПИСОК ЛИТЕРАТУРЫ

1. **Шавнев А.А., Курбаткина Е.И., Косолапов Д.В.** Методы соединения алюминиевых композиционных материалов (обзор) // Материалы и технологии, 2017, № 3 (48), стр. 35-42.
2. **Крылов Д.С., Назаров С.В.** Некоторые особенности аргонодуговой сварки алюминиево-магниевых сплавов // В сборнике: Актуальные проблемы авиации и космонавтики, Сборник материалов VI Международной научно-практической конференции, посвященной Дню космонавтики, в 3-х томах под общей редакцией Ю.Ю. Логинова, 2020, стр. 466-467.
3. **Drits A.M., Ovchinnikov V.V.** Weldability and properties of welds of high-strength aluminum alloys of the Al - Cu - Li system // Metal Science and Heat Treatment, 2012, V. 53, № 9-10, pp. 445-449.
4. **Овчинников В.В., Дриц А.М.** Сварка трением с перемешиванием алюминиевых сплавов с дополнительным охлаждением соединения // Электрометаллургия, 2021. № 10, стр. 2-14.
5. **Овчинников В.В., Березина В.А., Скакова Т.Ю.** Механические свойства соединений алюминиевых сплавов, выполненных сваркой трением с, при статическом и динамическом нагружении // Наукоемкие технологии в машиностроении, 2021, № 11 (125), стр. 20-29.
6. **Лаптев Е.А., Михайлицын С.В., Беляев А.И.** Сварка трением с перемешиванием алюминиевых сплавов // Актуальные проблемы современной науки, техники и образования, 2013, Т. 1, № 71.стр. 377-379.
7. **Drits A.M., Ovchinnikov V.V.** Properties of the joints of sheets of 1565ch alloy in combination with other aluminum alloys that were performed by friction welding with mixing // Russian Metallurgy (Metally), 2016, V. 2016, № 6, pp. 537-546.
8. **Amirov A.I., Beloborodov V.A., Ivanov A.N., Zhukov L.L.** Lap welded joint of aluminum and titanium alloy by friction stir welding // Collection of AIP Conference Proceedings, Proceedings of the Advanced Materials with Hierarchical Structure for New Technologies and Reliable Structures, 2018, 020013.
9. **Милютин В.С., Близник М.Г. Катаев Р.Ф.** Теория и технология контактной сварки // Екатеринбург, изд-во Уральского университета, 2015, 255 стр.

10. **Маликов А.Г., Оришич А.М., Витошкин И.Е., Карпов Е.В., Анчаров А.И.** Лазерная сварка разнородных материалов на основе термически упрочняемых алюминиевых сплавов // Прикладная механика и техническая физика, 2021, Т. 62, № 5 (369), стр. 161-171.
11. **Wang Z., Shao X., Bu X., Oliveira J.P., Zeng Z., Peng B.** Laser beam oscillating welding of 5a06 aluminum alloys: microstructure, porosity and mechanical properties // Optics & Laser Technology, 2019, V. 11, pp. 58-65.
12. **Кучук А.В.,-Яценко С.И., Чвертко П.Н., Семёнов Л.А., Гущин К.В. Самотрясов С.М.,** Контактная стыковая сварка изделий из высокопрочных сплавов на основе алюминия // Автоматическая сварка, 2013, № 7 (723), стр. 3-7.
13. **Чвертко П.Н., Семенов Л.А., Гущин К.В.** Контактная стыковая сварка оплавлением тонкостенных профилей из термически упрочняемых алюминиевых сплавов // Автоматическая сварка, 2014, № 12 (738), стр. 37-40.
14. **Dimitrescu A., Alecusan A.M., Babiş C., Chivu O., Ungureanu L.** Alternative non-demountable assembly technologies for aluminium alloy // In collection of 18th International Multidisciplinary Scientific GeoConference SGEM 2018., Conference proceedings, 2018, pp. 17-24.
15. **Гуреева М.А., Грушко О.Е., Клочков Г.Г.** Исследование свойств сварных соединений алюминиевого сплава В1341, выполненных контактной точечной сваркой // Заготовительные производства в машиностроении. 2016, № 7, стр. 8-12.
16. **Hasan I.Kh., Pan'kin N.A., Kyashkin V.M.** Xrd study of the surface of aluminum alloy AK5M7 after electric-spark alloying // Letters about materials, 2021, V. 11. № 1 (41), pp. 84-89.
17. **Korgin A.V.** Strength of aluminum alloy joints made by contact capacitor welding Vol. 19 No. 2 (2023): International Journal for Computational Civil and Structural Engineering, pp. 42-50.
18. Универсальная электромеханическая машина Instron 3382, Руководство пользователя, Instron, USA, 2015, 235 стр.
19. **НИЛ ИИМСК НИУ МГСУ** Технический отчет для АО «Русал ТД» «Разработка свода правил «Мосты с конструкциями из алюминиевых сплавов. Правила проектирования // НИУ МГСУ, Москва, 2020, 230 стр.
20. **WWW.Ans.Com.ru** Руководство по основным методам проведения анализа в программе ANSYS, https://vestnik.bsau.ru/netcat_files/File/CIT/manuals/ANSYS.pd, pp. 15-111.
21. **Анисимов А.Г., Ахмед С.М.** Экспериментальное исследование и численное моделирование метания алюминиевого образца для магнитно-импульсной сварки // Наука и инновации, 2022, № 3 (123), стр. 58-62.
22. **Максимов Н.Н., Сергеев В.Ю.** Совершенствование технологического процесса контактной сварки деталей из алюминиевых сплавов // Аллея науки, 2017, Т. 4, № 10, стр. 150-157.
23. **Андреева Л.П., Овчинников В.В., Сидоров А.А.** Оптимизация размеров точечных соединений при электроконтактной сварке алюминиевых сплавов // Современные материалы, техника и технологии, 2015, № 3 (3), стр. 23-32.

Korgin Andrey Valentinovich, Doctor of Technical Sciences, Professor, Professor of the Department of Testing Structures of the National Research Moscow State University of Civil Engineering (NRU MGSU), Moscow, 129337, Yaroslavskoye sh., 26. e-mail: korguine@mgsu.ru , anvakorg@gmail.com. tel. +7 495 183-54-29 (office) +7 985 765-46-38 (mobile)

Коргин Андрей Валентинович, Доктор технических наук, профессор, профессор кафедры испытаний сооружений Национального Исследовательского Московского Государственного Строительного Университета (НИУ МГСУ), Москва, 129337, Ярославское ш., д.26. e-mail: korguine@mgsu.ru, anvakorg@gmail.com. тел. +7 495 183-54-29 (раб.) +7 985 765-46-38 (моб.)